20024284(JSAE)
2002-32-1791(SAE)

Combustion Characteristics of a Direct Injection Stratified Charge Rotary Engine Using Spark Ignition and Pilot Flame Ignition Systems

(1) (2)
Takumi MUROKI, Yasuo MORIYOSHI, and Masahide TAKAGI

(1) (2)
Kanagawa Institute of Technology, Chiba University

A Direct Injection Stratified Charge Rotary Engine (DISC-RE) with a pilot flame ignition system which has high ignition energy, large flame contact area and long duration of ignition source, has been examined comparing with a spark ignition system, using a model combustion chamber simulating a DISC-RE. As a result, it was found that the combustion using the pilot flame ignition system was activated and that a better ignitability was attained under lean mixture conditions than using a spark ignition system. To analyze these experimental results, numerical calculations of the mixture formation and combustion process were carried out. Numerical analyses proved that the pilot flame ignition system was superior to the spark ignition system as the pilot flame ignition made large-area ignition source and large inflammable mixture region. Finally, a single rotor with 650 cc displacement DISC-RE was built as a prototype. Basic running tests of this engine under light load conditions were performed. Test results showed that capabilities of practical use with a higher thermal efficiency than conventional rotary engines.

***Key Words*: Rotary Combustion Engine, Stratified Charge Combustion / Pilot Flame Ignition, Glow Plug, Numerical Analysis, Indicated Thermal Efficiency**

1. INTRODUCTION

Applications of the stratified combustion system to a Wankel-type rotary engine have been carried out [1-5]. In rotary engines, because spark plugs or injectors cannot protrude into combustion chamber as the rotor rotates on the trochoid surface and very strong squish flow exists, a stable ignition system is indispensable. Thus, the authors have carried out analyses of the stratified charge combustion system using a pilot flame ignition system from experimental and theoretical aspects [6-9]. As compared with the spark ignition, the pilot flame ignition system allows a large ignition energy release and a large flame contact area with mixture as well as long flame contact duration. Therefore, the pilot flame ignition system is expected to provide a strong and reliable ignition source.

As the first step, a model combustion chamber has been employed in our study to simulate the physical phenomena in a real combustion chamber at around the ignition timing, because optical access is difficult using an actual engine. High speed photography and indicated pressure analyses were performed to evaluate both the spark ignition system and pilot flame ignition system.

After that to investigate these experimental results, numerical simulations were also carried out to analyze the mixture formation and the following combustion processes.

Finally, a small prototype of DISC-RE with the pilot flame ignition system was designed and built, then some basic tests were performed using light oil. .

2. EXPERIMENTAL METHOD

2.1 Test Apparatus Using a Model Combustion Chamber

In a Wankel rotary engine, since the combustion chamber rotates, it is somewhat difficult to make measurements inside the combustion chamber. Therefore, a fixed model combustion chamber, where approximately similar air velocity, pressure fields and chamber wall temperature to those of a real engine were realized, was employed as shown in Fig. 1. In order to supply the air into the model

combustion chamber, a two-stroke diesel engine was operated as a rapid compression and expansion machine under motored conditions. Two check valves were utilized to create uniflow inside the chamber, since uniflow is a feature of the Wankel rotary engine. The temperature of the model chamber wall was maintained at 523 K by using electric heaters. The fuel injection system comprised two injectors; a pilot injector which generated the pilot flame using a glow plug and a main injector which supplied fuel for the main combustion, as shown in the model combustion chamber. These specification are shown in Table 1. Combustion was controlled to occur once in consecutive five engine-cycles to remove the influence of previous combustion cycle. The test fuel adopted was JIS#2 light oil.

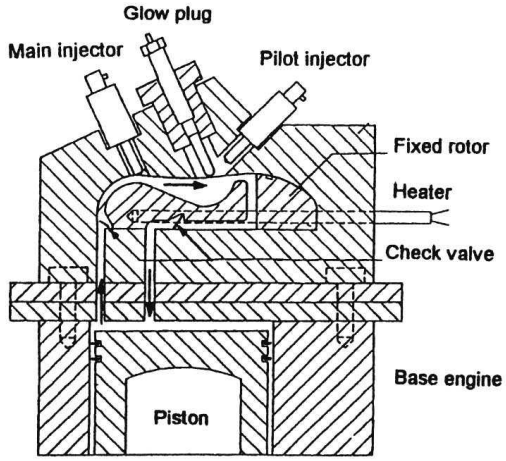


Fig. 1 Schematic of model combustion chamber

Table 1 Specifications of model chamber

Chamber volume [cc]		46
Dimension [width x length] [mm]		60 x 80
Effective compression ratio		7.4
Base engine speed [r/min]		473
Equivalent rotary engine speed [rpm]		1420
Diameter of nozzle [mm]	Pilot	1 x ϕ0.28
	Main	7 x ϕ0.15
Glow plug [length x diameter] [mm]		22 x f5
Spark plug gap [mm]		1.1

2.2 Flow Patterns inside the Model Combustion Chamber

To confirm a correlation between the flow patterns inside the combustion chamber of a real engine and the model combustion chamber, measurements of gas velocity inside the chamber were carried out. To measure the gas velocity inside the chamber, a Laser Doppler Velocimetry (LDV) fiber optic probe was employed. Shown in Fig.2 is the spatial distribution of mean velocity and r.m.s. turbulence velocity at 40 deg. BTDC, 20 deg. BTDC and TDC [11]. The mean velocity, $\overline{U}$, and the turbulence intensity, $\overline{u}'$, in the X and Y directions which are indicated as horizontal and vertical segments, respectively, are shown in this figure.

At 40 deg. BTDC, the horizontal flow direction is positive along the upper wall and a clockwise swirl flow exists near the center of the chamber. There is also a horizontally negative flow along the bottom wall, while turbulence is nearly isotropic around the center of the chamber but suppressed near the wall. At TDC, the mean velocity is generally low and the observed clockwise rotational flow decays and becomes imperceptible, while the turbulence intensity slightly decreases and approaches homogeneous and isotropic.

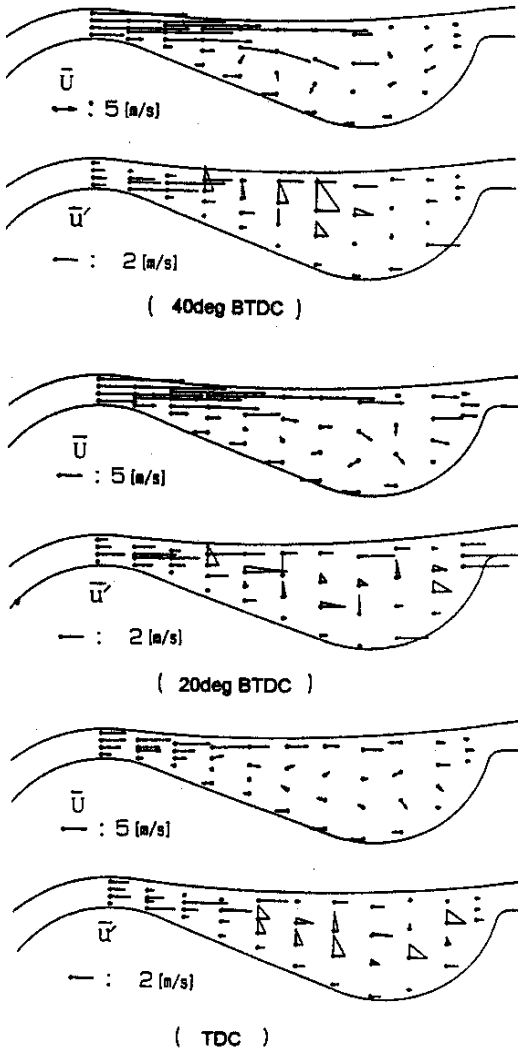


Fig. 2 Measured gas velocity inside the chamber

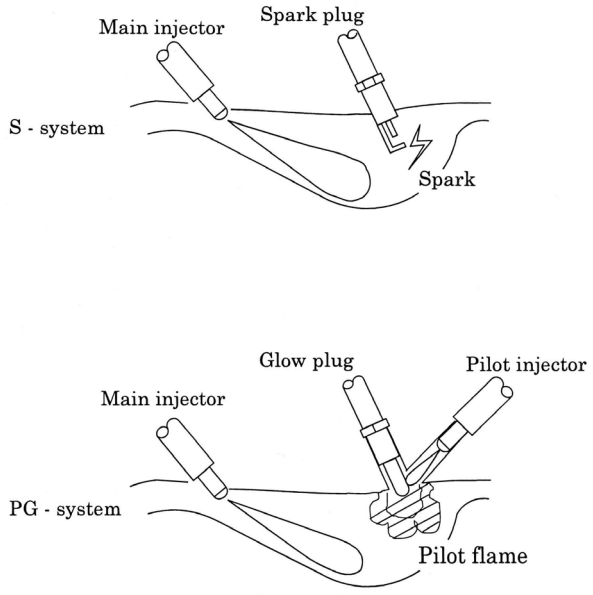


Fig. 3 Definition of ignition system

2.3 Ignition Systems

In this study, two ignition systems were employed for the experiment, as shown in Fig. 3.

(1) Spark ignition system (S-system)

Pilot injection was not employed in this system. A spark plug was used as the ignition source to ignite the spray from a main injector.

(2) Pilot flame ignition system (PG-system)

This ignition system employed a glow plug instead of a spark plug. By placing its tip close to a trochoid surface, the glow plug ignited the spray from the pilot injector to generate a pilot flame which subsequently ignited the main spray.

Methods of fuel supply differed, according to the ignition system. In this study, an injection quantity, Q_{Tinj}, was defined as follows.

$$Q_{Tinj} = Q_{Pinj} + Q_{Minj}$$

where, Q_{Pinj} and Q_{Minj} are the pilot and main injection quantities, respectively. Therefore, in the case of the S-system, which does not use pilot injection, the injection quantity, Q_{Tinj}, is equal to a main injection quantity, Q_{Minj}.

2.4 Indicated Pressure Analysis

For the indicated pressure analysis, pressure was detected by a piezo-type pressure transducer. Data were obtained at every crank angle and analyzed by ensemble averaging the data for 96 consecutive combustion cycles. From the averaged pressure value, an apparent rate of heat release that does not account for the heat loss was calculated.

2.5 Direct Photography Using a High-Speed Video Camera

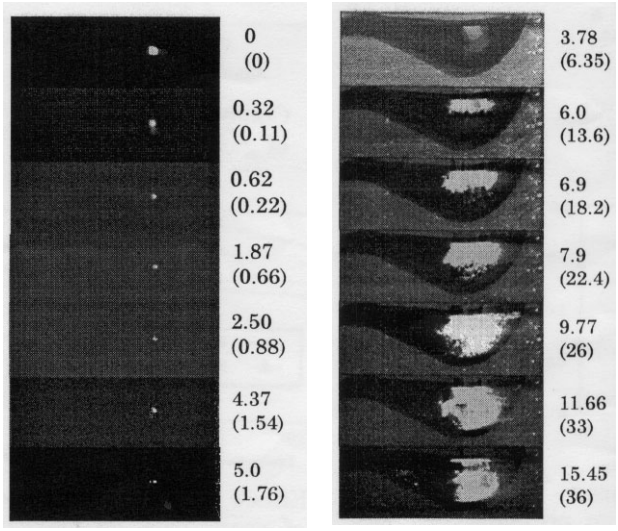
One of the side walls of the model combustion chamber was replaced with quartz. This allowed direct photographing of spark generation and flame inside the model chamber using a high-speed video camera (9000 fps).

3. TEST RESULTS

3.1 Ignition Energy Release Process

The process of ignition energy release was photographed using a high speed camera. Shown in Fig.4(a) is an example of the spark generation process at the ignition timing 27 deg. BTDC. From the image obtained, it was found that the spark duration was nearly 1.8 ms and accumulated heat release does not exceed 100 mJ.

Shown in Fig.4(b) is an example of the pilot flame generation process with injection timing of 13 deg. BTDC and injection amount of 3.5 mm^3/cycle.



(a) spark system
upper: time after ignition (deg.),
(lower): time after ignition (ms)

(b) pilot ignition system
upper: time after start of injection (deg.),
(lower): accumulated apparent heat release (J)

Fig. 4 High-speed photographs of two ignition

Compared to the spark ignition case, it is obvious that the pilot flame releases much more heat soon after ignition and that it attains large flame contact area and long flame contact duration (>5 ms).

3.2 Main Combustion Characteristics

3.2.1 Combustion pressure and heat release rate

In this test, the total injection quantity was set equal for the two systems, in order to make a

comparison of combustion characteristics between them. The results are shown in Fig.5. In the case of low injection quantity, Q_{Tinj}, from 10 to 12.5 mm^3/cycle, the PG-system yielded higher combustion pressure and rate of heat release than the S-system. However, when the injection quantity was increased to 16 mm^3/cycle, resulting in a rich mixture, the difference in combustion performance was disappeared

Fig.	Combustion system	Inj. amount (Q_{Minj}+Q_{Pinj}) (mm^3/cycle)	Ignition timing	Equivalence ratio(ϕ)
(a)	------- S_{30}	10+0	27CA° BTDC	0.30
	—— PG	6.5+3.5	——	
(b)	------- S_{30}	12.5+0	27CA° BTDC	0.38
	—— PG	9+3.5	——	
(c)	------- S_{30}	16+0	27CA° BTDC	0.49
	—— PG	12.5+3.5	——	

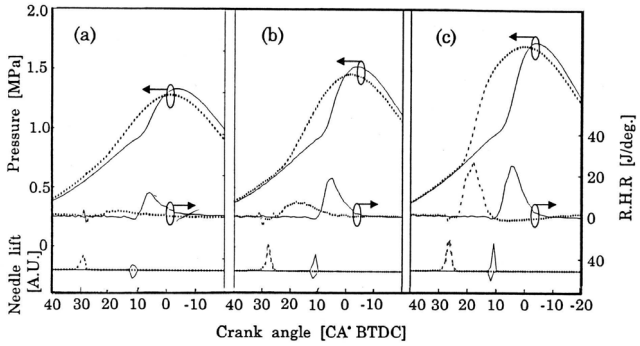


Fig. 5 Comparison of combustion characteristics between S-system and PG system

3.2.2 Misfire rate

As shown in Fig. 6, the misfire rate rapidly increased when the injection quantity was reduced to 12.5 mm^3/cycle or below in the S-system. On the contrary, in the PG-system, no misfire occurred over the whole range of injection quantity, because the pilot flame ignition allowed stable combustion for a wide range of mixture rate. However, when the injection amount reached 14.5 mm^3/cycle, little or no difference of misfire rate could be found between the two ignition systems.

3.2.3 Fuel mass burnt velocity

The apparent fuel mass burnt velocity, M g/s, was examined for two combustion durations of 5-10 and 10-20 percent fuel mass fraction burnt. Figure 7 is the result in each range. It was found that the S-system had a considerably lower fuel mass burnt velocity than the PG-system for a low injection quantity. However, the velocity of the S-system came closer to that of the PG-system as the injection quantity increased and finally became nearly equal to that of the PG-system when the injection quantity was increased to 16 mm^3/cycle.

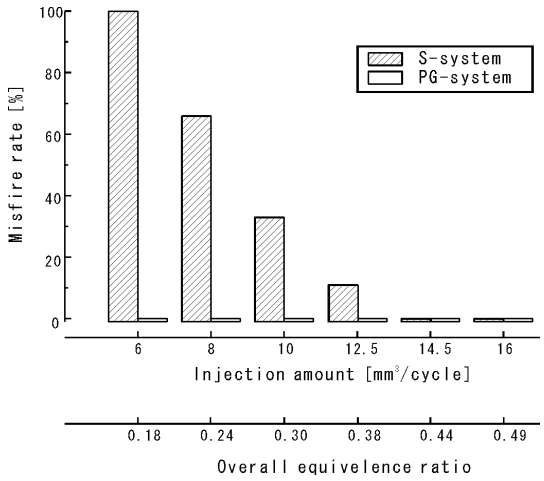


Fig. 6 Misfire rate vs. injection amount for both S- and PG-systems

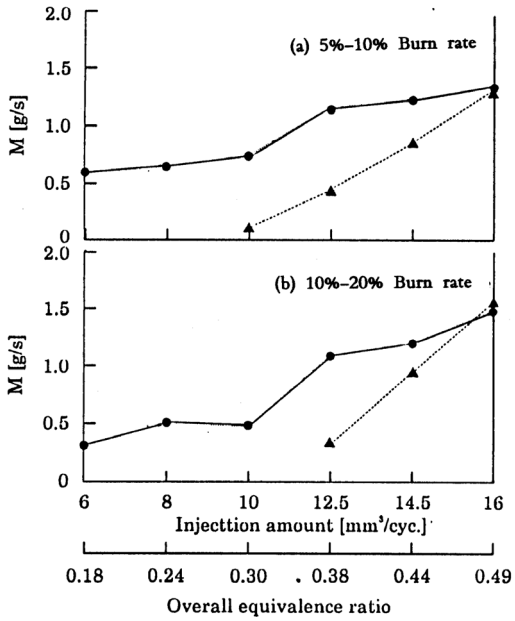


Fig. 7 Effect of injection quantity on fuel mass burnt velocity, M
(●:PG-system, ▲: S-system)

3.2.4 Direct photographs of the combustion process

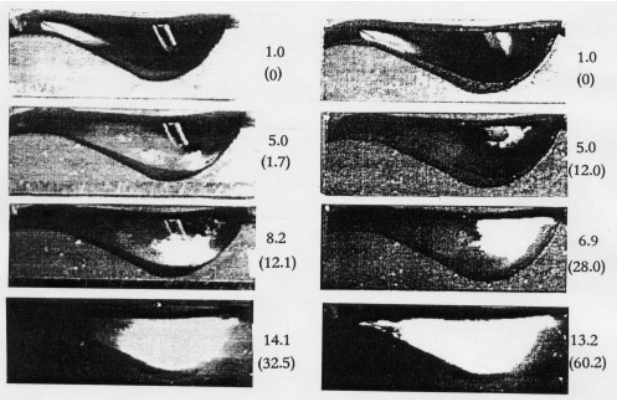
Setout in Fig. 8 are high-speed photographs of the combustion process for the different ignition systems, where the injection quantity, Q_{Tinj}, was maintained at 10 mm^3/cycle for both systems.

In the S-system, the flame kernel was generated at the position of the electrode, then the flame expanded and propagated into the rich mixture area at the bottom of the chamber, however, combustion flame did not reach the trailing corner of combustion chamber. On the contrary, in the PG-system, a pilot

flame was generated at a stagnation area behind the glow plug. The flame expanded to the leading corner of the combustion chamber and propagated into the rich mixture area at the bottom of the chamber, then propagating into the trailing corner. Finally, the luminescence filled the whole area of the combustion chamber.

From these pictures, it is evident that the pilot flame ignition activates the main combustion.

In production engines, flame propagation to the leading (upwind) side is sometimes prevented by the strong squish flow due to the one-way rotation. Adopting the PG-system may overcome this defect.



(a) S-system (b) PG-system

Fig. 8 High speed photographs of combustion process (upper: time after start of injection (deg.), (lower): accumulated apparent heat release (J))

4. NUMERICAL ANALYSIS IN MODEL COMBUSTION CHAMBER

4.1 Calculation Method

In order to predict the mixture-formation process and the following combustion process, a commercial code of "Fluent" (Ver. 4.5) was employed with some additional implementations. A spray model with droplet breakup, droplet vaporization, and wall-impingement sub-models was introduced [10]. The k-ε turbulence model and Magnussen's combustion models were also used. Only the part of combustion chamber was cut out of the model engine as the calculation region. Because the chamber geometry is symmetrical to the vertical center-surface, calculations were made in the half volume. The pressure values at both the inlet and outlet cross sections were given based on experimental values while the initial velocity field was given using LDV measured data [7]. The number of the total meshes is 27500. Calculations were carried out from start of injection timing (13 deg. BTDC) to 6 deg. ATDC. As fuel, n-tetradecane, a major component of light oil, was assumed.

In the case of PG-system, pilot injection started at 13 deg. BTDC for 3.15 deg. with fuel amount of 3.5 mm^3/cycle, while main injection started at 13 deg. BTDC for 3.45 deg. with fuel amount of 9.0 mm^3/cycle, and the surface temperature of glow plug was kept constant at 1200 K. In the case of S-system, only main injection started at 13 deg. BTDC for 6.20 deg. with fuel amount of 12.5 mm^3/cycle, and two ignition cells were set at the location of spark gap and its temperature was kept at 2500 K from 10 deg. BTDC to 7 deg. BTDC.

4.2. Calculated Results

The results of all calculated droplet parcels projected onto a vertical plane, and the spatial distributions of equivalence ratio and velocity vectors on both the vertical center-cross-section and horizontal cross-section at 7 deg. BTDC are shown in Fig. 9. Also, the spatial distributions of gaseous temperature on both the vertical center-cross-section and horizontal cross-section are shown in Fig. 10. In the early ignition stage at 6 deg. BTDC, a larger flame kernel is formed in PG-system than in S-system. Also, the mixture distribution seems larger in PG-system than in S-system at 7deg. ATDC due to enhanced gas motion caused by pilot flame jet. The temporal change of gaseous temperature is more drastic in PG-system than in S-system especially after TDC.

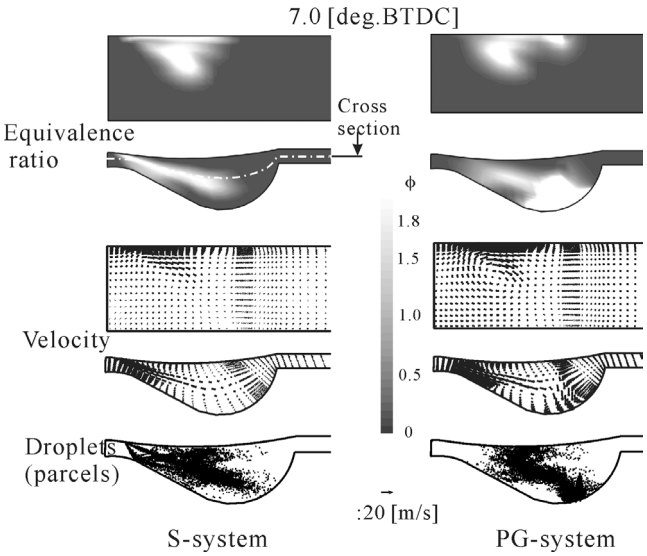


Fig. 9 Spatial distributions of equivalence ratio and velocity vectors on vertical and horizontal cross sections and projected parcels of droplets

Figure 11 shows the spatial distribution of kinetic turbulence energy at -1deg. ATDC. Much higher turbulence energy is available in PG-system due to the quick combustion caused by strong ignition source. It should be noted that the spread of high temperature region is not dispersed, but continually

changing because the unburned gaseous temperature is not so high to occur spontaneous ignition.

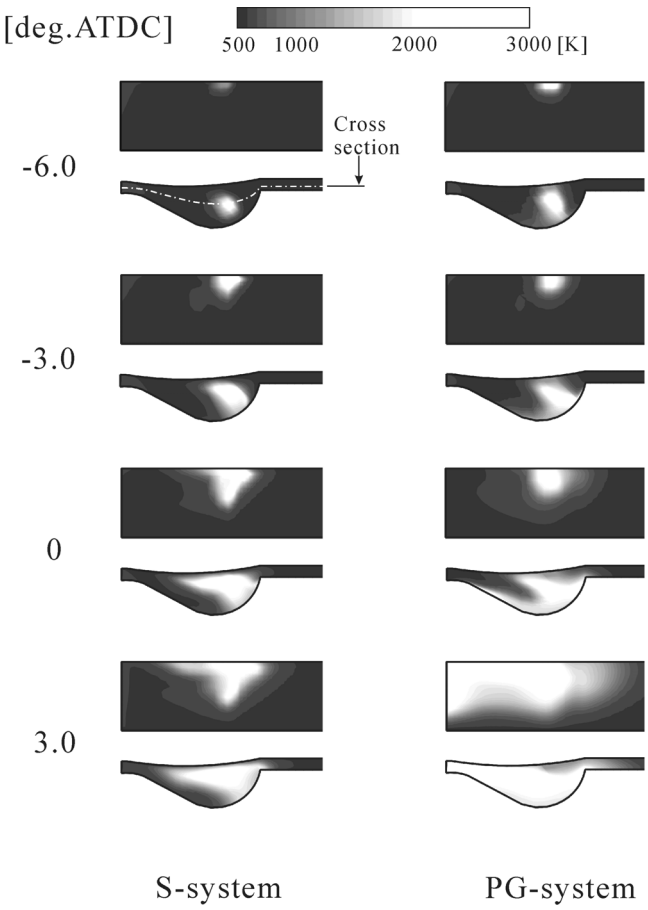


Fig. 10 Spatial distributions of temperature on center-vertical and horizontal cross-sections

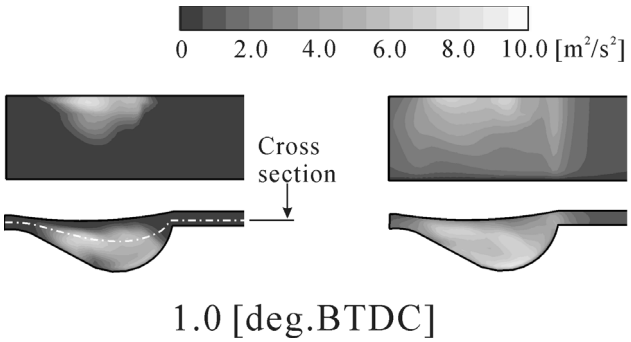


Fig. 11 Spatial distribution of turbulence kinetic energy on center vertical and horizontal cross-sections

The results of accumulated heat release amount for both the calculation and measurement are indicated in Fig. 12. Fairly good agreement is found in the early combustion stage. The PG-system shows significantly activate combustion compared to the S-system.

Thus, numerical analyses proved that the PG-system is superior to the S-system as the pilot injection makes wide-area ignition source, wide-spread inflammable mixture region due to the enhanced gas motion, and strong turbulence energy caused by the quick combustion.

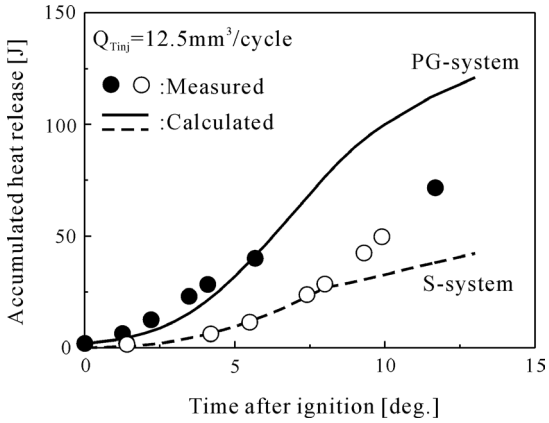


Fig. 12 Temporal variations of accumulated heat release amount after ignition for calculation and measurement

5. BASIC PERFORMANCE TESTS OF A PROTOTYPE DISC-RE

5.1 Proto-Type DISC-RE Engine

A prototype DISC-RE with a single rotor, which was modified from a two-rotor production rotary engine, was built as shown in Fig. 13. Fuel injection system comprised two distributed-type fuel pumps and two injectors of pilot and main injections as shown in Fig. 1. The engine specifications are listed in Table 2.

Engine performance tests were performed using the indicated-pressure analysis. The indicated mean effective pressure, IMEP, P_i, and indicated specific fuel consumption, ISFC, b_i, are obtained using a strain-type pressure transducer which was set near the injectors to measure the gas pressure near TDC.

Because the intake, compression and expansion, and exhaust strokes cannot be measured using a single transducer in a rotary engine, the unmeasured pressure value was estimated assuming polytropic changes. Engine speed was set constant at 1500 r/min. As fuel, JIS #2 light oil was used. The coolant water and lubricant oil temperatures were set at 348 K.

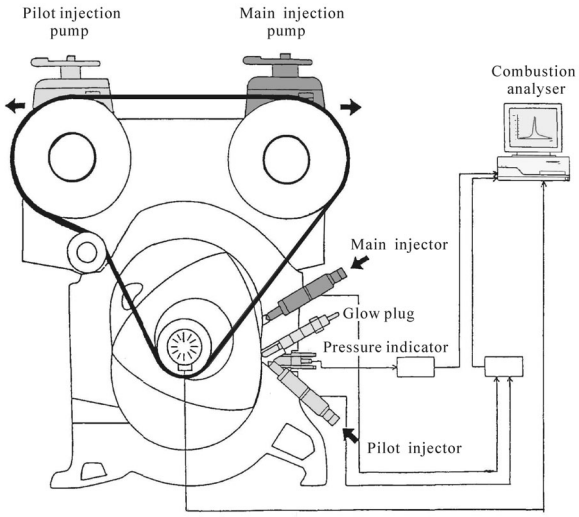


Fig. 13 Prototype of DISC-RE

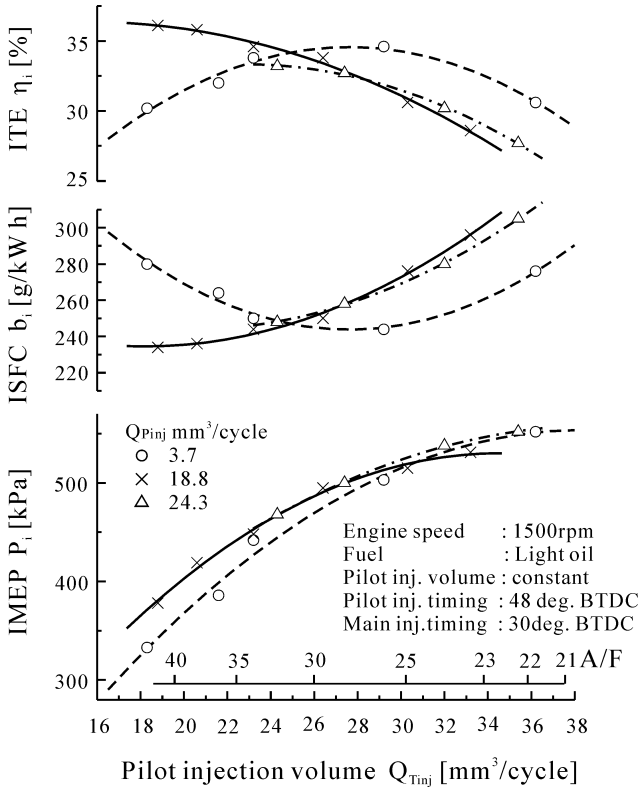


Fig. 14 Performance characteristics vs. fuel injection quantity with pilot and main injections

5.2 Test Results

The pilot injection volume, Q_{Pinj}, was set at 3.7, 18.8, or 24.3 mm^3/cycle.

The performance results are shown in Fig. 14. At light load conditions, the best ISFC was obtained with Q_{Pinj} = 18.8 mm^3/cycle, while it was derived with Q_{Pinj} = 3.7 mm^3/cycle at higher load conditions. In higher load conditions, thermal efficiency became worse, although the A/F ratio was still larger than the stoichiometric value. This is due to that mixing is not enough and rich mixture takes much time to burn.

To improve the thermal efficiency and output performance in high load conditions, using a turbo-charger or unifying mixture distribution inside the chamber would be required.

Table 2 Engine specifications

Engine		Rotary Engine
Displacement		654 cc × 1 rotor
Compression ratio		9.4 : 1
Port timing	I.O. I.C. E.O. E.C.	45 deg. ATDC 50 deg. ABDC 75 deg. BBDC 50 deg. ATDC
Fuel injection pump	Type Inj.press.	Distributor type 13 MPa
Injection nozzle	Pilot inj. Main inj.	1× ϕ 0.28 mm 7× ϕ 0.15 mm
Injection timing	Pilot inj. Main inj.	48 deg. BTDC 30 deg. BTDC
Glow plug		9 Volt × 10.5 Amp.

6. CONCLUSIONS

1. The test results using the model combustion chamber proved that as the pilot flame ignition system activates the main combustion, especially in the lean mixture conditions, better combustion stability, rapid combustion, and higher heat release are obtained compared with spark ignition system.

2. The reason above results was examined by numerical analyses. The PG-system is superior to the S-system as the pilot injection has much thermal energy and makes wide-area ignition source, widely-spread inflammable mixture region due to the enhanced gas motion, and strong turbulence energy caused by the quick combustion.

3. A prototype DISC rotary engine with the pilot flame ignition system was designed and built. Engine basic performance test were carried out. In relatively light load conditions (IMEP less than 450 kPa), better ISFC was obtained than a conventional rotary engine. To improve performance in high load condition, using a turbo charger or unifying mixture distribution inside the chamber would be required.

REFERENCES

[1] C. Jones, and H. Lamping, C.W. Development Status of DISC-RE, SAE Paper 710582, 1971.
[2] H. L. Nguyen, H.E. Addy, Performance and Efficiency Evaluation and Heat Release Rate Study of DISC-RE, SAE Paper 870445, 1987.
[3] H. J. Shock, and J. S. Stageman, Calculation of the Unsteady 3-D Flow Field inside a Motored DISC-RE, SAE Paper 880625, 1988.
[4] J. Abraham, and F. V. Bracco, Comparisons of Computed and Measured Mean Velocity and Turbulent Intensity in a Motored R.E., SAE Paper 881602, 1988.
[5] Y. Hasegawa, and K. Yamaguchi, An Experimental Investigation on Air-Fuel Mixture Formation Inside a Low Pressure DISC-RE, SAE Paper 930678, 1993.
[6] T. Muroki, S. Gotou, and K. Morita, A study of an outline of combustion for a direct injection stratified charge rotary engine. SAE Paper 901600, 1990.
[7] Y. Moriyoshi, T. Muroki, and W. Xu., A study on combustion characteristics of DISC rotary engine using a model combustion chamber. SAE Paper 941028, 1994.
[8] Y. Moriyoshi, T. Muroki, and Y. W. Song, Stratified charge combustion system using pilot flame ignition. Trans. of JSME (in Japanese), 61-950B, 1998, 1566.
[9] T. Muroki and Y. Moriyoshi, Combustion characteristics of spark-ignition and pilot flame ignition systems in a motored Wankel stratified charge engine, J. of Automobile Engineers, 214-D, 2000, 949.
[10] Y. Moriyoshi, M. Takagi, and X. Hu, Analysis of Mixture Formation Process with a Swirl-Type Injector, SAE Paper 2000-01-2057, 2000
[11] Y. Moriyoshi, T. Muroki, and W. Xu, A Study on Combustion Characteristics of DISC Rotary Engine Using a Model Combustion Chamber, SAE Paper No. 941028